

**GROWTH AND CHARACTERIZATION OF DICOUMAROLE DERIVATIVE****S. K. Parmar<sup>1</sup>, H. K. Gohil<sup>2</sup>, P. M. Vyas<sup>3</sup>, S. D. Hadiyal<sup>4</sup> and A. H. Patel<sup>5</sup>**Research Scholar<sup>1,2</sup>, Assitant Professor<sup>3</sup>, Associate Professor<sup>5</sup>, Department of Physics, Kamani Science College & Prataprai Arts College, AmreliResearch Scholar<sup>4</sup>, Department of Chemiustry, Saurashtra University, Rajkot**ABSTRACT**

The Dicoumarole derivative 4-amino-3-((4-amino-2-oxo-2H-chromen-3-yl)(3-(4-chlorophenyl)-1-phenyl-1H-pyrazol-4-yl)methyl)-2H-chromen-2-one obtain by crystal growth by slow evaporation solution growth method having approximate dimensions of 0.630 x 0.400 x 0.310 mm. The Crystal where characterized using different characterization techniques like single crystal XRD, FT-IR, dielectric study, TG-DTA and UV-Visible spectra. Single crystal XRD was adopted for determination of lattice constant, space group and structure analysis. FT-IR spectrum denotes that there are mainly six group of absorption. The dielectric study represent that dielectric constant decreased as the frequency of the applied field increased and also studied The variation of dielectric loss, a.c. conductivity and a.c. resistivity with frequency of the applied field in the frequency range from 20 Hz to 2 MHz at room temperature. Thermal stability of dicoumarole determine by TG-DTA study. The study of UV-Visible spectrum denotes that the good transmittances of the crystal in the entire visible region.

*Keywords:* Dicoumarole crystal, solution growth, single Crystal XRD, FT-IR, Dielectric, TG-DTA, UV-Visible spectrum.

**INTRODUCTION**

A significant number of the known coumarins are fluorescent particles and they are known to have great quantum yield [6, 15] and high photo stability [2, 4]. The coumarins are mostly colorless but substitutions at various positions bring out a red shift in absorption and emission, and are utilized in the applications such as laser dyes [16], textile dyes [5], sensors [14] as a optical brighteners [13], non-linear optical (NLO) materials [17] and in biological labeling [11, 22]. The mixes with azo usefulness are less fluorescent to non-fluorescent in nature. Azo practical gathering at the 3-position of 4-hydroxy coumarins particle was first reported by Yazdanbaksh et al. [23]. In the later studies on these molecules, UV-visible absorption, fluorescence and acid dissociation constants were reported [23, 21]

The synthesis of Dicoumarole 4-amino-3-((4-amino-2-oxo-2H-chromen-3-yl)(3-(4-chlorophenyl)-1-phenyl-1H-pyrazol-4-yl methyl)-2H-chromen-2-one crystal growth by slow evaporation solution growth method. A colorless block crystal of C<sub>36</sub>H<sub>29</sub>ClN<sub>4</sub>O<sub>5</sub>S having approximate dimensions of 0.630 x 0.400 x 0.310 mm was obtains. The single crystal XRD study reveals that of dicoumarole derivative has primitive triclinic crystal system, Based on a statistical analysis of intensity distribution, and the successful solution and refinement of the structure, the space group was determined to be: P-1 (#2). FT-IR spectrum represent that there are mainly six groups of absorption are Alcohol, Alkene, Alkyl halide, Amine, Aromatic and Ether. The dielectric study of dicoumarole derivative was done in the frequency range from 20 Hz to 2 MHz at room temperature. The dielectric constant decreased as increased the frequency of the applied field. The variation of dielectric loss, a.c. conductivity and a.c. resistivity also studied with the frequency of the applied field. Increasing frequency of applied field the dielectric constant and dielectric loss decreased and the a.c. conductivity was due to the correlated barrier hopping. The TGA study shows that sample remain stable up to 200°C. The DTA curve shows a major endothermic peak at 284.29°C which correspond to the melting point of material. The sharpness of peak at 284.29°C indicates the high purity of the grown crystal. The study of optical transmittance spectrum of the grown crystal is shows that there is no appreciable absorption of light in the entire visible region. The good transmittance property of the crystal was found in the entire visible region.

**SYNTHESIS OF MATERIAL AND CRYSTAL**

4-amino coumarin (0.01mol) was taken in methanol (20 ml) and refluxed for few min. till clear solution was observed. Then pyrazole aldehyde (0.005 mol), 2-3 drops of conc. HCl and reflux the reaction mixture for 10 hours. The completion of reaction was monitored by Thin Layer Chromatography System, solvent system ethyl acetate: hexane (8:2). After completion of the reaction, the reaction mixture was cooled and poured over ice water (50 ml). The solid crude product, was filtered, washed with water and dried to give the desired compound.

Pure compound 4-amino-3-((4-amino-2-oxo-2H-chromen-3-yl)(3-(4-chlorophenyl)-1-phenyl-1H-pyrazol-4-yl)methyl)-2H-chromen-2-one was taken in 20 ml with binary mixture of DMSO+IPA and heated till compound completely dissolve. Then 0.5 gm charcoal was added and further it was heated to remove

color impurity. The hot solution was filtered through wattmann 41 filter paper. The solution was allowed to cool gradually and kept in a stopper conical flask slightly opened. The crystal was grown up due to thin layer evaporation. Reaction scheme of dicoumarole derivative is shown in figure 1.

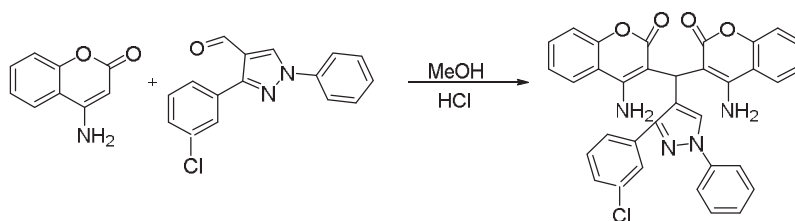


Fig.-1: Reaction scheme of dicoumarole derivative

## RESULT AND DISCUSSION

### A. Single crystal X-Ray Diffraction

Single-crystal X-ray diffraction is most commonly used for precise determination of a unit cell, including cell dimension and position of atoms within the lattice. Bond-length and angle are directly related to the atomic position. The crystal structure of a mineral is a characteristic property that is the basis for understanding many of the properties of each mineral.

A colorless block crystal of  $C_{36}H_{29}ClN_4O_5S$  having approximate dimensions of 0.630 x 0.400 x 0.310 mm was mounted on a glass fiber. All measurements were made on a Rigaku SCX mini diffractometer using graphite monochromatic Mo-K $\alpha$  radiation. The crystal-to-detector distance was 52.00 mm. Cell constants and an orientation matrix for data collection corresponded to a primitive triclinic cell with dimensions:

$$a = 10.2924(7) \text{ \AA} \quad \alpha = 74.321(2)^\circ$$

$$b = 11.9363(8) \text{ \AA} \quad \beta = 84.571(3)^\circ$$

$$c = 13.8467(9) \text{ \AA} \quad \gamma = 89.790(3)^\circ$$

$$V = 1630.0(2) \text{ \AA}^3$$

For  $Z = 2$  and F.W. = 665.16, the calculated density is 1.355 g/cm<sup>3</sup>. Based on a statistical analysis of intensity distribution, and the successful solution and refinement of the structure, the space group was determined to be:

P-1 (#2)

The data were collected at a temperature of  $20 \pm 1^\circ\text{C}$  to a maximum  $2\theta$  value of  $55.0^\circ$ . A total of 540 oscillation images were collected. A sweep of data was done using  $\omega$  oscillations from  $-120.0$  to  $60.0^\circ$  in  $1.0^\circ$  steps. The exposure rate was 10.0 [sec./ $^\circ$ ]. The detector swing angle was  $-30.80^\circ$ . A second sweep was performed using  $\omega$  oscillations from  $-120.0$  to  $60.0^\circ$  in  $1.0^\circ$  steps. The exposure rate was 10.0 [sec./ $^\circ$ ]. The detector swing angle was  $-30.80^\circ$ . Another sweep was performed using  $\omega$  oscillations from  $-120.0$  to  $60.0^\circ$  in  $1.0^\circ$  steps. The exposure rate was 10.0 [sec./ $^\circ$ ]. The detector swing angle was  $-30.80^\circ$ . The crystal-to-detector distance was 52.00 mm. Readout was performed in the 0.146 mm pixel mode. Crystal Structure of dicoumarole molecules is shown in figure 2, Oak Ridge Thermal-Ellipsoid Plot diagram of molecule is shown in figure 3, PLATON ellipsoid plot diagram of molecule is shown in figure 4 and packing diagram of dicoumarole is shown in figure 5. Detail analysis in crystal data form of dicoumarole by Single crystal XRD is shown in table-1.

**Table-1: Analysis of Single Crystal XRD of Dicoumarole**

Empirical Formula	$C_{36}H_{29}ClN_4O_5S$
Formula Weight	665.16
Crystal Color, Habit	colorless, block
Crystal Dimensions	0.630 X 0.400 X 0.310 mm
Crystal System	Triclinic
Lattice Type	Primitive
Lattice Parameters	$a = 10.2924(7) \text{ \AA}$
	$b = 11.9363(8) \text{ \AA}$
	$c = 13.8467(9) \text{ \AA}$
	$\alpha = 74.321(2)^\circ$
	$\beta = 84.571(3)^\circ$
	$\gamma = 89.790(3)^\circ$
	$V = 1630.0(2) \text{ \AA}^3$

Space Group	P-1 (#2)
Z value	2
D <sub>calc</sub>	1.355 g/cm <sup>3</sup>
F000	692.00
μ(MoKα)	2.308 cm <sup>-1</sup>

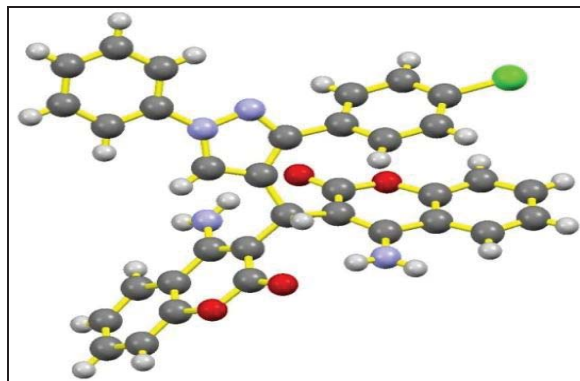


Fig.-2: Crystal structure of molecules

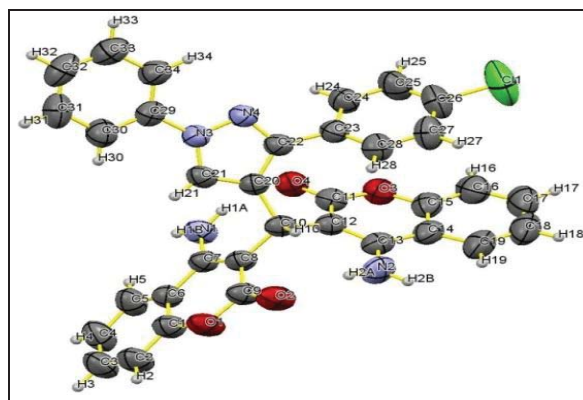


Fig.-3: Oak ridge thermal-ellipsoid plot diagram of molecule

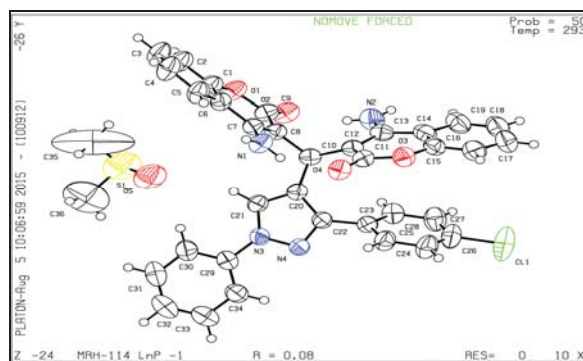


Fig- 4: Platon ellipsoid plot diagram of molecule

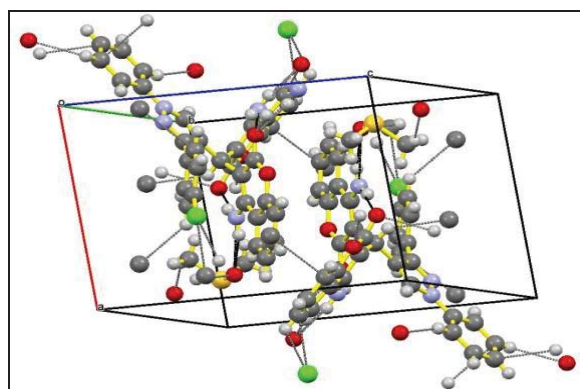


Fig.-5: Packing Diagram of dicoumarole derivative

## B. FT-IR Study

The study of infrared spectra involves examination of stretching, bending and vibration mode of atoms in molecules. Hence it is useful to determination of functional group of samples.

Figure 6 shows FT-IR spectrum of 4-amino-3-((4-amino-2-oxo-2H-chromen-3-yl)(3-(4-chlorophenyl)-1-phenyl-1H-pyrazol-4-yl)methyl)-2H-chromen-2-one crystal. There are mainly six groups of absorption. The detail analysis of the FT-IR spectrum of dicoumarole is given in table 2.

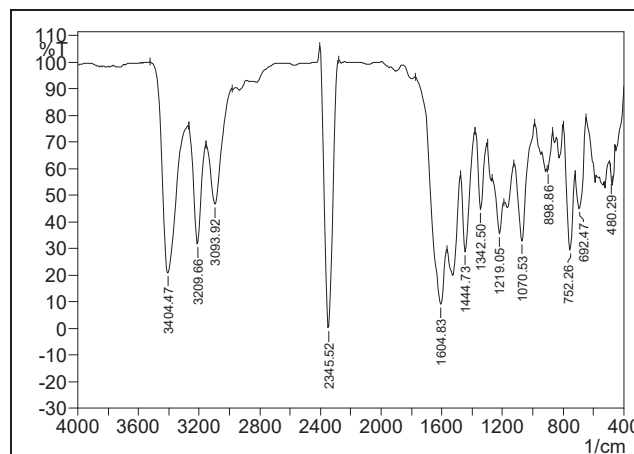


Fig.-6: FT-IR Spectrum of dicoumarole

Table-2: Analysis of FT-IR Spectrum of Dicoumarole

Type	Validation Mode	Type of Vibration	Absorption peaks( $\text{cm}^{-1}$ )
Alcohol	O-H	Stretch	3209.66
Alkenes	=C-H	Stretch	3093.92
	C=C	Stretch	1604.83
	=C-H	Bending	898.86
Alkyl halide	C-Cl	Stretch	752.26
	C-Cl	Stretch	692.47
Amine	N-H	Stretch	3404.47
	C-N	Stretch	1342.5
	C-N	Stretch	1219.05
Aromatic	C=C	Stretch	1444.73
Ether	C-O	Stretch	1070.53

## C. Dielectric Study

The dielectric constant is one of the basic electrical properties of solids. Dielectric properties are correlated with the electro-optic property of the crystals (Aithal et al., 1997). The capacitance ( $C_p$ ) and dielectric loss ( $\tan \delta$ ) of 4-amino-3-((4-amino-2-oxo-2H-chromen-3-yl)(3-(4-chlorophenyl)-1-phenyl-1H-pyrazol-4-yl)methyl)-2H-chromen-2-one crystal were measured using the conventional parallel plate capacitor method for at room temperatures with frequency ( $f$ ) range of 20Hz to 2 MHz .

Dielectric study of Active Pharmaceutical Ingredients, amino acids and carbohydrates has been reported [8]. A broadband dielectric spectroscopic investigation of Verapamil Hydrochloride (VH), a calcium channel blocker by Adrjanowicz et al. [12] is carried out to understand its molecular dynamics. The dielectric investigation of amorphous pharmaceutical drugs has been reported in correlation with molecular mobility and isothermal crystallization kinetics [9].

For the most part there are four contributions playing important role in the value of dielectric constant ( $\epsilon'$ ); which are from electronic, ionic, dipolar and space-charge polarizations. All these may be active in low frequency region. The nature of the variation of  $\epsilon'$  with frequency recommended which contribution is prevailing. The space-charge contribution based on the purity and perfection of the crystal

Figure 7 shows the change of  $\epsilon'$  with frequency of applied field. The dielectric constant decreases very quickly as frequency increases. The nature of the plot in the figure 7 recommended that the space-charge polarization is active in low frequency region, which is reflected in terms of very quickly decrease in the value of dielectric constant with increase in frequency. This also further recommended that the dipoles can not comply with the

varying field and hence the decreasing nature is exhibited, which is a common feature in 4-(2-hydroxyphenylamino)-pent-3-en-2-one [3] and zinc tartrate crystals [18]. More-or-less, the same type of nature is observed for the change in dielectric loss ( $\tan\delta$ ) with the frequency of applied field as shown in the figure 8. Recently, an a.c. conductivity and dielectric constant measurements of bulk pyronine G (Y) is reported by Yaghmour [20]. The author notice that the dielectric constant and dielectric loss decreased by increasing frequency and the a.c. conductivity was because of the correlated barrier hopping.

Generally, typical current carriers in organic solids are through  $\pi$ - conjugated systems and the electrons can change position via  $\pi$ -electron cloud, especially, by hopping, tunneling and other associated mechanisms. Figure 9 shows that the a. c. conductivity  $\sigma_{ac}$  increases as the frequency increases and the completely different nature is observed for a. c. resistivity. In case of the a. c. conductivity if the angular frequency of applied field is represented by

$$\omega = 2\pi\nu$$

The Jonscher's equation [1, 10] can be written as follows,

$$\sigma_{ac}(\omega, T) = \sigma_{dc}(T) + a(T)\omega^n$$

Where,  $\sigma_{dc}(T)$  (or static,  $\omega=0$ ) is the dc conductivity because of excitation of electrons from a localized state to the conduction band,  $a(T)\omega^n$  is the ac conductivity because of the dispersion phenomena occurring in the material,  $a(T)$  is a temperature dependent constant and  $n$  is the power law exponent, which generally change between 0 and 1 depending on temperature. The exponent  $n$  represents the degree of interaction between mobile ions with the lattice around them. A typical frequency dependence of conductivity spectrum shows three distinguish regions, namely, (a) low frequency dispersion, (b) an intermediate frequency plateau and (c) an extended dispersion at high frequency.

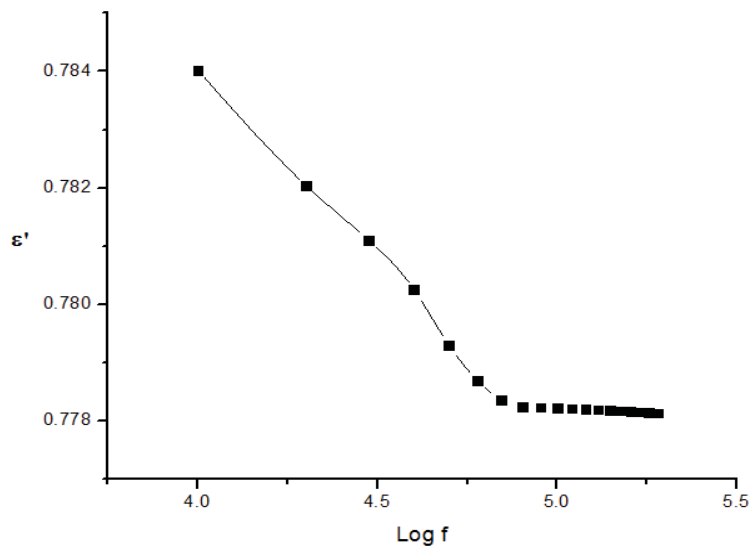


Fig.-7: Plot of dielectric constant versus log f.

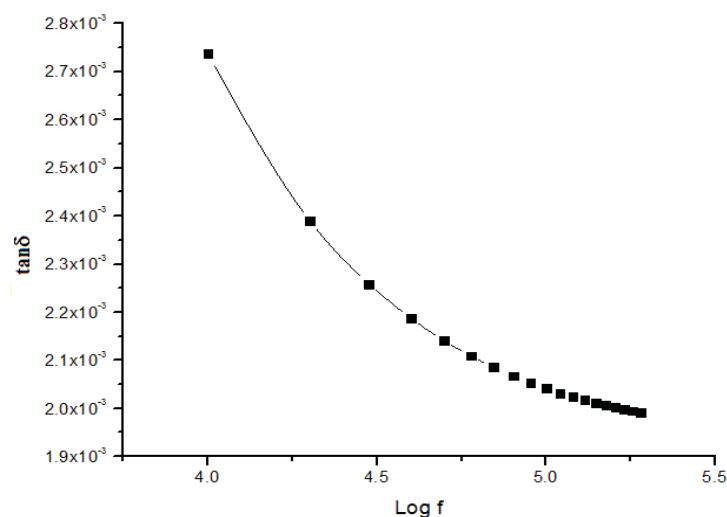


Fig.-8: Plot of dielectric loss versus log f.

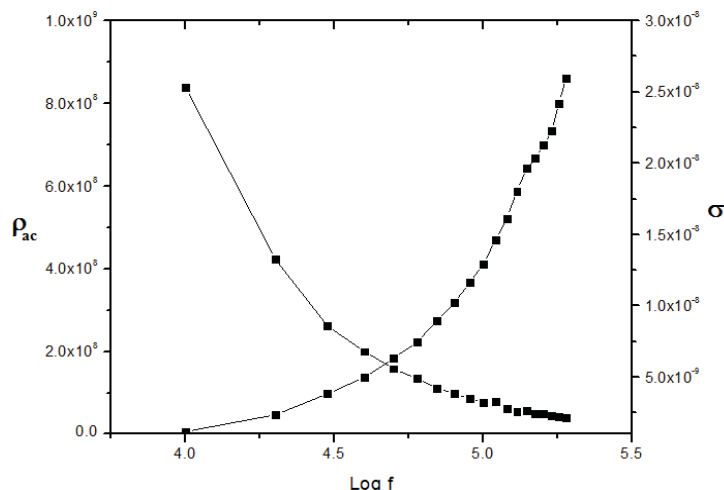


Fig.-9: Plot of a. c. conductivity and a. c. resistivity versus log f.

#### D. Thermo gravimetric analysis

Thermo gravimetric and differential thermal analysis gives information regarding thermal stability, weight loss of compound, phase transaction and different stage of decomposition of the crystal system. Figure 10 shows the thermo gram of simultaneous recorded TGA and DTA. The thermo gravimetric analysis of dicoumarole is carried out between 30<sup>o</sup>C to 800<sup>o</sup>C in nitrogen atmosphere at a heating rate of 10<sup>o</sup>C/min.

The TGA plot shows that sample remain stable up to 200<sup>o</sup>C. The DTA curve shows a major endothermic peak at 284.29<sup>o</sup>C which correspond to the melting point of material. The sharpness of peak at 284.29<sup>o</sup>C is indicating the high purity of the grown crystal. The absence of water in molecular structure is indicated by absence of weight loss around 100<sup>o</sup>C.

The TGA curve shows that there are three state of weight loss. The first weight loss is about at 200<sup>o</sup>C. Which is indicates the beginning of the decomposition. Second stage of weight loss was occurring between 300<sup>o</sup>C and 450<sup>o</sup>C. Weight loss above 450<sup>o</sup>C is assign to the decomposition of the compound.

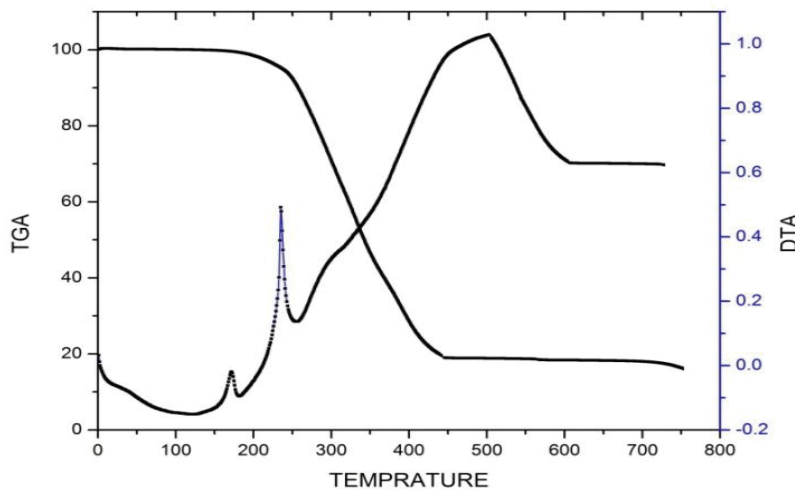


Fig.-10: Plot of TG-DTA of dicoumarole derivative crystal

#### E. UV-Visible spectra

Ultraviolet and visible spectroscopy is mainly used to determine the amount of conjugated double bond in the molecules. Most organic compounds with variable functional groups are transparent in the range of the electromagnetic spectrum, which we call ultraviolet (UV) and visible (Vis.) regions. In electromagnetic spectrum, the UV comes in range of 100–400 nm.

The UV spectra of dicoumarole were recorded on a Shimadzu- 1700 UV spectrophotometer using N,N-Dimethylformamide as solvents with concentration of solution is  $1.4 \times 10^{-7}$  mmol. The optical transmittance spectrum of the grown crystal is shown in figure 11. and it indicates that there is no appreciable absorption of light in the entire visible region. The good transmittance property of the crystal in the entire visible region was

ensuring its stability for second harmonic generation applications [19]. Figure 11 shows the plot of absorption and transmittance versus wave length of UV-Visible radiation in the range of 100 nm to 800 nm.

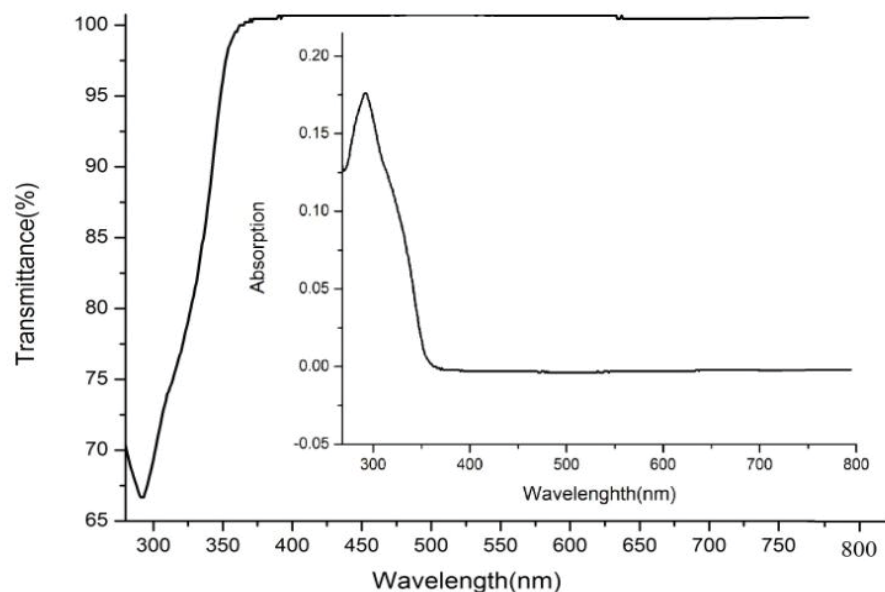


Fig.-11: Plot of UV-Visible spectrum of dicoumarole derivative

## CONCLUSION

The synthesis of Dicoumarole 4-amino-3-((4-amino-2-oxo-2H-chromen-3-yl)(3-(4-chlorophenyl)-1-phenyl-1H-pyrazol-4-yl)methyl)-2H-chromen-2-one crystal growth by slow evaporation solution growth method. having approximate dimensions of 0.630 x 0.400 x 0.310 mm. Based on a statistical analysis of intensity distribution, and the successful solution and refinement of the structure, the space group was determined to be: P-1 (#2). FT-IR spectrum shows there are mainly six groups of absorption found are Alcohol, Alkene Alkyl halide, Amine, Aromatic and Ether. The dielectric study was carried out in the frequency range from 20 Hz to 2 MHz at room temperature. The dielectric constant decreased as the frequency of the applied field increased. The variation of dielectric loss, a.c. conductivity and a.c. resistivity also studied with frequency of the applied field the dielectric constant and dielectric loss decreased by increasing frequency and the a.c. conductivity was due to the correlated barrier hopping. The studies of TGA plot shows that sample remain stable up to 200°C. The DTA curve shows a major endothermic peak at 284.29°C which correspond to the melting point of material. The sharpness of peak at 284.29°C is indicating the high purity of the grown crystal. The absence of water in molecular structure is indicated by absence of weight loss around 100°C. The study of UV-Visible spectrum of the grown crystal indicates that there is no appreciable absorption of light in the entire visible region. The good transmittance property of the crystal in the entire visible region was ensuring its stability for second harmonic generation applications.

## ACKNOWLEDGMENTS

The authors are thankful to Department of physics Saurashtra University - Rajkot and Sophisticated instrumentation center (SICART), Vallbh Vidhyanagar for grant the permission for analysis facility.

## REFERENCES

1. A. K. Jonscher, Nature.267, 673 (1977).
2. Azzouz IM, Salah A (2012) nonlinear optical absorption and NIR to blue conversion in highly stable polymeric dye rod. Appl Phys B 108:469–474. doi:10.1007/s00340-012-4915-y
3. B. Parekh, D. H. Purohit, P. Sagayraj, H. S. Joshi, and M. J. Joshi, Cryst. Res. Technol.42, 407 (2007)
4. Chen J, Liu W, Zhou B et al (2013) Coumarin- and rhodaminefused deep red fluorescent dyes: synthesis, photophysical properties, and bioimaging in vitro. J Org Chem 78:6121–6130. doi:10.1021/jo400783x
5. Christie RM, Morgan KM, Islam MS (2008) Molecular design and synthesis of N-arylsulfonated coumarin fluorescent dyes and their application to textiles. Dye Pigment 76:741–747. doi:10.1016/j.dyepig.2007.01.018

6. Cigáň M, Donovalová J, Szöcs V et al (2013) 7-(Dimethylamino)coumarin-3-carbaldehyde and its phenylsemicarbazone: TICT excited state modulation, fluorescent H-aggregates, and preferential solvation. *J Phys Chem A* 117:4870–4883. doi:10.1021/jp402627a
7. Enakshi and K. V. Rao, *J. Mater. Sci. Lett*4, 1298 (1985).
8. R. Mantheni, M. P. K. Maheswaran, H. F. Sobhi, N. I. Perea, A. T. Riga, M. E. Matthews, and K. Alexander, *J. Term. Anal. Calorim.*, DOI: 10.1007/s10973-011-1423-y.
9. J. Menegotto, J. Alie, C. Lacabanne, and M. Bauer, *Dielectric News Lett.*19, 1 (2004).
10. J. O. López and R. G. Aguilar, *Rev. Mex. Fis.*49, 529 (2003).
11. Jung HS, Kwon PS, Lee JWJHJY et al (2009) Coumarin-derived Cu(2+)-selective fluorescence sensor: synthesis, mechanisms, and applications in living cells. *J Am Chem Soc* 131:2008–2012. doi: 10.1021/ja808611d
12. K. Adrjanowicz, K. Kaminski, M. Paluch, P. Włodarczyk, K. Grzybowska, Z. Wojnarowska, L. Hawelek, W. Sawicki, P. Lepek, and R. Lunio, *J. of Pharma. Sci.*99, 828 (2010).
13. Keskin SS, Aslan N, Bayrakçeken F (2009) Optical properties and chemical behavior of Laser-dye Coumarin-500 and the influence of atmospheric corona discharges. *Spectrochim Acta A Mol Biomol Spectrosc* 72:254–259. doi:10.1016/j.saa.2008.09.024
14. Kim T-K, Lee D-N, Kim H-J (2008) Highly selective fluorescent sensor for homocysteine and cysteine. *Tetrahedron Lett* 49:4879–4881
15. Krzeszewski M, Vakuliuk O, Gryko DT (2013) Color-tunable fluorescent dyes based on benzo[c]coumarin. *Eur J Org Chem* 5631–5644. doi:10.1002/ejoc.201300374
16. Nedumpara RJ, Thomas KJ, Jayasree VK et al (2007) Study of solvent effect in laser emission from Coumarin 540 dye solution. *Appl Opt* 46:4786. doi:10.1364/AO.46.004786
17. Painelli A, Terenziani F (2001) Linear and non-linear optical properties of push-pull chromophores: vibronic and solvation effects beyond perturbation theory. *Synth Met* 124:171–173. doi:10.1016/S0379-6779(01)00431-3
18. R. M. Dabhi, B. B. Parekh, and M. J. Joshi, *Ind. J. Phys.*79, 503 (2005).
19. S. Dhanuskodi, K. Vasantha, P.A.A. Mary, Structural and thermal characterization of a semiorganic NLO material: l-alanine cadmium chloride. *Spectro. Acta Part A*66,637–642 (2007)
20. S. J. Yagmour, *Eur. Phys. J. Appl. Phys.* 49, 10402 (2010).
21. Shahinian EGH, Haiduc I, Sebe I (2011) Synthesis and characterization of new azo coumarin dyes. *UPB Sci Bull Ser B Chem Mater Sci* 73:153–160
22. Sheng R, Wang P, Gao Y et al (2008) Colorimetric test kit for Cu<sup>2+</sup> detection. *Org Lett* 10:5015–5018. doi:10.1021/ol802117p
23. Yazdanbakhsh MR, Ghanadzadeh A, Moradi E (2007) Synthesis of some new azo dyes derived from 4-hydroxy coumarin and spectrometric determination of their acidic dissociation constants. *J Mol Liq* 136:165–168. doi:10.1016/j.molliq.2007.03.005